Spatiotemporal characterization of single-order high harmonic pulses from time-compensated toroidal-grating monochromator

Motohiko Ito,[1] Yoshimasa Kataoka,[1] Tatsuya Okamoto,[1] Mikio Yamashita,[1,2] and Taro Sekikawa[1,*]

[1] *Department of Applied Physics, Hokkaido University, Kita-13, Nishi-8, Kita-ku, Sapporo 060-8628, Japan*
[2] *CREST, Japan Science and Technology Agency, Sanbancho 5, Chiyoda-ku, Tokyo 102-0075, Japan*
**sekikawa@eng.hokudai.ac.jp*

Abstract: Extreme ultraviolet (XUV) single-order high harmonic pulses with 10^6 photons/pulse were separated from multiple harmonic orders by a time-compensated toroidal-grating monochromator consisting of a pair of toroidal gratings. The first grating separates the harmonic order and the second one compensates for the pulse-front tilt. The center photon energies were tunable between 42 and 23 eV. The separated single harmonic pulses were spatially and temporally characterized as having a spot size of 58 ± 3 μm at the focus, with a shortest pulse duration of 47 ± 2 fs. The developed XUV light source is versatile for application to time- and space-resolved spectroscopy.

OCIS codes: Multiharmonic generation; (320.7100) Ultrafast measurements; (190.4160).

References and links

1. H. C. Kapteyn, O. Cohen, I. Christov, and M. Murnane, "Harnessing attosecond science in the quest for coherent X-rays," Science **317**(5839), 775–778 (2007).
2. F. Krausz, and M. Ivanov, "Attosecond physics," Rev. Mod. Phys. **81**(1), 163–234 (2009).
3. M. Nagasono, E. Suljoti, A. Pietzsch, F. Hennies, M. Wellhöfer, J.-T. Hoeft, M. Martins, W. Wurth, R. Treusch, J. Feldhaus, J. R. Schneider, and A. Föhlisch, "Resonant two-photon absorption of extreme-ultraviolet free-electron-laser radiation in helium," Phys. Rev. A **75**(5), 051406 (2007).
4. A. Baltuška, T. Udem, M. Uiberacker, M. Hentschel, E. Goulielmakis, Ch. Gohle, R. Holzwarth, V. S. Yakovlev, A. Scrinzi, T. W. Hänsch, and F. Krausz, "Attosecond control of electronic processes by intense light fields," Nature **421**(6923), 611–615 (2003).
5. Y. Nabekawa, T. Shimizu, T. Okino, K. Furusawa, H. Hasegawa, K. Yamanouchi, and K. Midorikawa, "Interferometric autocorrelation of an attosecond pulse train in the single-cycle regime," Phys. Rev. Lett. **97**(15), 153904 (2006).
6. P. M. Paul, E. S. Toma, P. Breger, G. Mullot, F. Auge, P. Balcou, H. G. Muller, and P. Agostini, "Observation of a train of attosecond pulses from high harmonic generation," Science **292**(5522), 1689–1692 (2001).
7. G. Sansone, E. Benedetti, F. Calegari, C. Vozzi, L. Avaldi, R. Flammini, L. Poletto, P. Villoresi, C. Altucci, R. Velotta, S. Stagira, S. De Silvestri, and M. Nisoli, "Isolated single-cycle attosecond pulses," Science **314**(5798), 443–446 (2006).
8. T. Sekikawa, A. Kosuge, T. Kanai, and S. Watanabe, "Nonlinear optics in the extreme ultraviolet," Nature **432**(7017), 605–608 (2004).
9. R. Haight, and D. R. Peale, "Tunable photoemission with harmonics of subpicosecond lasers," Rev. Sci. Instrum. **65**(6), 1853–1857 (1994).
10. T. Shimizu, T. Sekikawa, T. Kanai, S. Watanabe, and M. Itoh, "Time-resolved Auger decay in CsBr using high harmonics," Phys. Rev. Lett. **91**(1), 017401 (2003).
11. P. Wernet, M. Odelius, K. Godehusen, J. Gaudin, O. Schwarzkopf, and W. Eberhardt, "Real-time evolution of the valence electronic structure in a dissociating molecule," Phys. Rev. Lett. **103**(1), 013001 (2009).
12. L. Nugent-Glandorf, M. Scheer, D. A. Samuels, A. M. Mulhisen, E. R. Grant, X. Yang, V. M. Bierbaum, and S. R. Leone, "Ultrafast time-resolved soft x-ray photoelectron spectroscopy of dissociating Br2," Phys. Rev. Lett. **87**(19), 193002 (2001).
13. N. L. Wagner, A. Wüest, I. P. Christov, T. Popmintchev, X. Zhou, M. M. Murnane, and H. C. Kapteyn, "Monitoring molecular dynamics using coherent electrons from high harmonic generation," Proc. Natl. Acad. Sci. U.S.A. **103**(36), 13279–13285 (2006).
14. M. Uiberacker, T. Uphues, M. Schultze, A. J. Verhoef, V. Yakovlev, M. F. Kling, J. Rauschenberger, N. M. Kabachnik, H. Schröder, M. Lezius, K. L. Kompa, H.-G. Muller, M. J. J. Vrakking, S. Hendel, U. Kleineberg, U.

#121623 - $15.00 USD Received 16 Dec 2009; revised 3 Feb 2010; accepted 4 Mar 2010; published 11 Mar 2010

Heinzmann, M. Drescher, and F. Krausz, "Attosecond real-time observation of electron tunnelling in atoms," Nature **446**(7136), 627–632 (2007).
15. T. Sekikawa, T. Okamoto, E. Haraguchi, M. Yamashita, and T. Nakajima, "Two-photon resonant excitation of a doubly excited state in He atoms by high-harmonic pulses," Opt. Express **16**(26), 21922–21929 (2008).
16. P. Villoresi, "Compensation of optical path lengths in extreme-ultraviolet and soft-x-ray monochromators for ultrafast pulses," Appl. Opt. **38**(28), 6040–6049 (1999).
17. L. Nugent-Glandorf, M. Scheer, D. A. Samuels, V. M. Bierbaum, and S. R. Leone, "A laser-based instrument for the study of ultrafast chemical dynamics by soft x-ray-probe photoelectron spectroscopy," Rev. Sci. Instrum. **73**(4), 1875–1886 (2002).
18. L. Poletto, P. Villoresi, E. Benedetti, F. Ferrari, S. Stagira, G. Sansone, and M. Nisoli, "Intense femtosecond extreme ultraviolet pulses by using a time-delay-compensated monochromator," Opt. Lett. **32**(19), 2897–2899 (2007).
19. L. Poletto, P. Villoresi, E. Benedetti, F. Ferrari, S. Stagira, G. Sansone, and M. Nisoli, "Temporal characterization of a time-compensated monochromator for high-efficiency selection of extreme-ultraviolet pulses generated by high-order harmonics," J. Opt. Soc. Am. B **25**(7), B44–B49 (2008).
20. H. Mashiko, A. Suda, and K. Midorikawa, "Focusing coherent soft-x-ray radiation to a micrometer spot size with an intensity of 10(14) W/cm2," Opt. Lett. **29**(16), 1927–1929 (2004).
21. T. E. Glover, R. W. Schoenlein, A. H. Chin, and C. V. Shank, "Observation of laser assisted photoelectric effect and femtosecond high order harmonic radiation," Phys. Rev. Lett. **76**(14), 2468–2471 (1996).
22. J. M. Schins, P. Breger, P. Agostini, R. C. Constantinescu, H. G. Muller, A. Bouhal, G. Grillon, A. Antonetti, and A. Mysyrowicz, "Cross-correlation measurements of femtosecond extreme-ultraviolet high-order harmonics," J. Opt. Soc. Am. B **13**(1), 197–208 (1996).
23. L. Poletto, P. Villoresi, E. Benedetti, F. Ferrari, S. Stagira, G. Sansone, and M. Nisoli, "Intense femtosecond extreme ultraviolet pulses by using a time-delay-compensated monochromator: erratum," Opt. Lett. **33**(2), 140–140 (2008).
24. W. Becker, S. Long, and J. K. McIver, "Modeling harmonic generation by a zero-range potential," Phys. Rev. A **50**(2), 1540–1560 (1994).
25. M. Lewenstein, P. Salières, and A. L'Huillier, "Phase of the atomic polarization in high-order harmonic generation," Phys. Rev. A **52**(6), 4747–4754 (1995).
26. L. Poletto, "Tolerances of time-delay-compensated monochromators for extreme-ultraviolet ultrashort pulses," Appl. Opt. **48**(23), 4526–4535 (2009).
27. T. E. Glover, A. H. Chin, and R. W. Schoenlein, "High-order harmonic pulse broadening in an ionizing medium," Phys. Rev. A **63**(2), 023403 (2001).
28. Y. Kobayashi, T. Ohno, T. Sekikawa, Y. Nabekawa, and S. Watanabe, "Pulse width measurement of high-order harmonics by autocorrelation," Appl. Phys. B **70**(3), 389–394 (2000).

1. Introduction

The recent development of high harmonics, x-ray lasers, and free-electron lasers is providing us with unique opportunities to investigate nonlinear optics and ultrafast phenomena in the extreme ultraviolet (XUV) and soft x-ray regions [1–3]. Among these opportunities, high harmonics, which are generated by the interaction between ultrashort laser pulses and rare gases, appear to be promising for spectroscopy because of the compactness of their experimental apparatus and their ultrashort temporal durations that break into the attosecond regime [4–8]. High harmonics can now realize the direct observation of the dynamics in atoms, molecules, and solid-state materials with femtosecond and attosecond temporal resolution [9–14].

However, we face some difficulties in the application of high harmonics to spectroscopy, especially time-resolved and nonlinear spectroscopy, since many multiple orders of high harmonics are generated coaxially along with intense fundamental laser pulses, and the target signals probed by an appropriate harmonic order are often covered with the noises caused by the other harmonic orders. For example, we have had difficulty detecting the very weak photoelectron signals created by the two-photon absorption of high harmonics, because the photoelectrons from one-photon absorption were very strong and partially covered the nonlinear signals [15]. This is due to the poor reflectance contrast of the multilayered mirror that is used for focusing the harmonics. The use of a grating offers, what is seemingly, the simplest solution to this problem. However, the diffraction on a grating introduces a pulse-front tilt because of the difference in the length of the optical paths inside the harmonic beam, and as a consequence, the pulse duration of the harmonic pulses becomes longer than 100 fs [9,11]. To remedy this difficulty, Villoresi proposed an optical system in which one selects a certain spectral region by the first grating with an exit slit and compensates for the pulse front tilt of the pulses with a second grating [16]. Figure 1(a) presents a schematic diagram of a

#121623 - $15.00 USD Received 16 Dec 2009; revised 3 Feb 2010; accepted 4 Mar 2010; published 11 Mar 2010

compensator that employs a pair of toroidal gratings. This optical configuration achieves not only the separation of the harmonic order but also the focusing of the harmonic pulses.

In this paper, we report the development of a pulse-front-tilt compensator, that is, a time-compensated toroidal-grating monochromator, based on this configuration, i.e. with a pair of toroidal gratings, and demonstrate the spatiotemporal characterization of single-order harmonic pulses separated by the compensator. Nugent-Glandorf *et al.* and Poletto *et al*. have already constructed similar time-compensated monochromators [17,18]. In the former case, the combination of a spherical grating and a toroidal grating was employed, but the use of a spherical grating in the grazing incident angle introduces a high degree of astigmatism. It therefore becomes inevitable that the profile of the output beam is greatly distorted and the throughput at the center slit becomes lower. For example, we conducted a ray-trace simulation under the condition described in Ref. 17. We also made a simulation with an assumption that a pair of the toroidal grating was used. Here, the gratings were assumed to be at the 0th order reflection. Figure 1(b) shows that the 100-μm circular beam profile is distorted into a bow-shape after passing through a harmonic compensator with a spherical grating, while a pair of toroidal gratings yields a circular profile with a diameter of 100 μm. In the case of the diffracted beam, the beam profiles should be worse than the results of the simulations. Therefore, a configuration that includes a pair of toroidal gratings should provide improved focusability. In the latter case [18], four toroidal mirrors and two plane gratings were used. Although the pulse duration was compressed to 8 fs and the total throughput of the time-compensated monochromator was increased by about 18% due to the conical diffraction gratings [18,19], the relatively complicated optical configuration is difficult to construct. Thus, because the simplicity of the original design proposed by Villoresi [16] still offers more practical advantages, we were motivated to evaluate it. In particular, we sought to characterize its focusability for the first time.

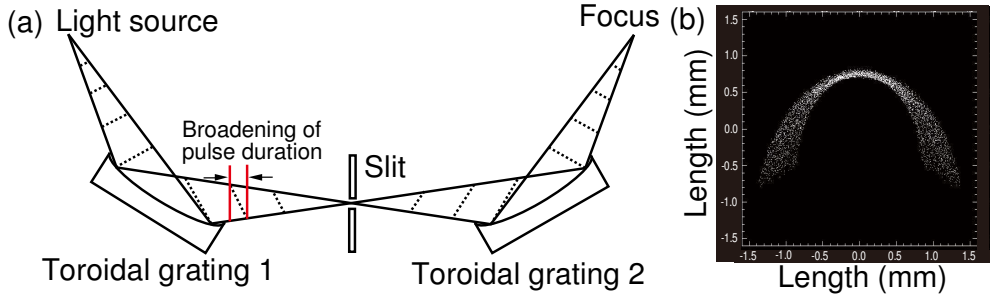

Fig. 1. (a) Schematic of a pulse-front-tilt compensator. The dotted lines indicate the pulse front inside the beam. The distance between the red lines corresponds to the broadening of the pulse duration. (b) Numerically simulated output beam profile of the compensator using the combination of a concave and a toroidal gratings. The spot size by a pair of toroidal gratings is about 100 μm in diameter.

2. Experiment

We characterized three features of the output pulses from the compensator: the pulse energies, the size of the focus spots, and the pulse durations of selected high harmonics. High harmonics were generated by focusing Ti:sapphire (TiS) laser pulses into a pulsed argon gas jet with a mirror having a 50-cm focal length. The TiS laser system delivered 800-μJ, 30-fs pulses at a repletion rate of 1 kHz. The laser pulses were separated in two by a beam splitter: 600-μJ pulses were used for high harmonic generation and the remaining pulses were for the probe used in the temporal characterization. The spot size of the laser beam for high harmonic generation was 68 μm and, then, the peak intensity was 5.5×10^{14} W/cm^2.

The pulse-front-tilt compensator, schematics of which are presented in Fig. 2, consists of a pair of toroidal gratings (HORIBA Jobin Yvon, 54000910) with radii of curvature of 1-m and 104.09-mm in the horizontal and vertical directions, respectively. Accordingly, the deviation angle is 142 degree. The groove density is 550 lines/mm with a variable pitch. The distances

#121623 - $15.00 USD Received 16 Dec 2009; revised 3 Feb 2010; accepted 4 Mar 2010; published 11 Mar 2010

from the center of the grating to the entrance and the exit foci are 319.9 and 319.5 mm, respectively. The spectral dispersions are 2.07 nm/mm at 48.75 nm and 2.22 nm/mm at 82.5 nm. The toroidal gratings were mounted on the rotational stages and were installed so that the emitting point of high harmonics coincided with the source point of the first toroidal grating. The slit that selects one harmonic order was placed at the image point of the first grating. The second grating, which compensates for the pulse-front tilt, was placed symmetrically with respect to the slit. A harmonic order was chosen by rotating the stage accessible from the outside of the vacuum chamber. The harmonic separator was very compact: the total optical path length from the emitting point of high harmonics to the focusing point was 1.28 m.

The selected harmonic order was monitored by a photoelectron spectrometer. The output fluence of high harmonic pulses was measured by a calibrated XUV photodiode (AXUV-100, IRD Inc.). To visualize the XUV photons, we employed a Ce:YAG crystal to convert them to visible photons of around 500 nm [20]. The luminescence from the Ce:YAG crystal inserted at the focal point was imaged on a CCD camera with a lens at a magnification of 1.3. Since the pixel size of the CCD camera was 7.4 μm × 7.4 μm, the uncertainty of the measured spot size was ± 2.8 μm. The temporal durations of the selected harmonic pulses were measured by observing the temporal evolution of the sideband peaks in photoelectron spectra of Ne that were caused by the two-photon free-to-free transition under the simultaneous irradiation of both XUV and fundamental photons [21,22]. The peak intensity of a probe pulse was 1.3×10^{11} W/cm^2, which is weak enough not to cause the ponderomotive shift in the photoelectron spectra. The photoelectrons were detected by a multichannel plate (MCP) after passing through a time-of-flight tube, and were then counted.

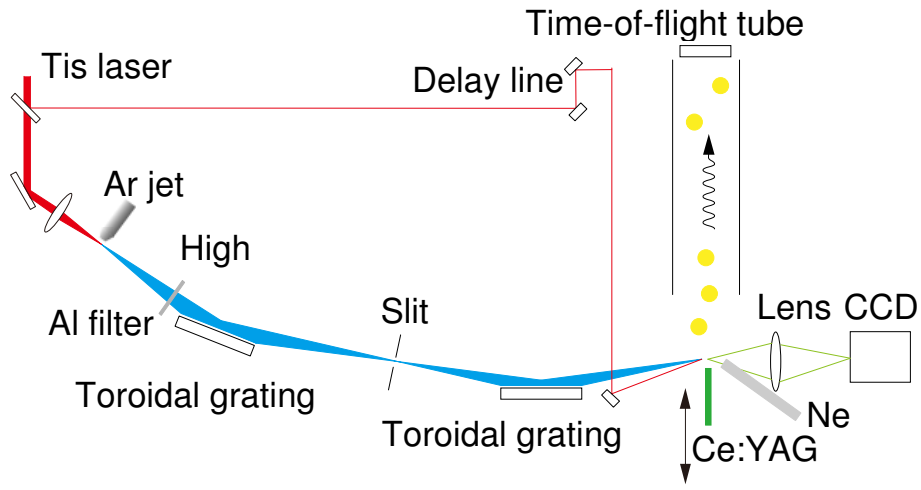

Fig. 2. Experimental setup for the spatial and temporal characterization of the pulse-front-tilt compensator. For the measurement of the beam profiles, a Ce:YAG crystal was inserted at the focal point.

3. Results and discussion

3.1 Pulse energy

The toroidal grating used has a maximum diffraction efficiency of 16% at 35 nm. Thus, the total throughput of the compensator is 2.6%. The final output pulse energies of the separated harmonics between the 15th and 29th harmonic are tabulated in Table 1. The maximum photon number was 4.2×10^6 photons/pulse at the 21st harmonic. The ambiguity of the photon number was approximately 10 percent. Compared with the results of previous works, we could obtain better results in the output photon numbers on target [17,23]. Since the repetition rate of the driving laser pulses was 1 kHz, the average fluence was on the order of

#121623 - $15.00 USD Received 16 Dec 2009; revised 3 Feb 2010; accepted 4 Mar 2010; published 11 Mar 2010

10^9 photons/s, which is almost comparable to the output of a small synchrotron radiation facility.

The improvement in the absolute photon numbers over Ref. 17 was achieved by employing a pair of toroidal gratings. By replacing a first spherical grating with a toroidal grating, the focal spot becomes smaller and then the throughput of separated harmonic pulses at the slit becomes higher. Therefore, in spite of the smaller input laser energy 600 μJ than 1.8 mJ in Ref. 17, more harmonic photons were focused on target. Compared with Ref. 23, the improvement was primarily achieved by increasing the pulse energy of the driving laser from 230 to 600 μJ. We also used a pulsed gas jet to supply dense gas for high harmonic generation. Consequently, although the total diffraction efficiency of the gratings employed here 2.6% is lower than the time-compensated monochromator 18% [18], the final extracted pulse energies were comparable. Our results therefore suggest that the optical system tested in this work has also attractive potential.

Table 1. Photon numbers at the focus point of the compensator

Harmonic order	Photon energy (eV)	Photon number per pulse ($\times 10^6$)
15	23.4	0.7
17	26.5	2.1
19	29.6	3.2
21	32.8	4.2
23	35.9	3.0
25	39.0	1.3
27	42.1	0.7
29	45.2	0.1

3.2 Spot size at the focal point

Since, in the XUV region, it is necessary to use all the optical components except for multilayer mirrors in the grazing incidence, we must take into account the astigmatisms in optical systems. A slight deviation from the design might lead to the distortion of a beam profile. Therefore, we measured the beam profiles of the output beams to confirm the focusability of the pulse-front-tilt compensator.

When both gratings were set to the 0th-order reflection, the output beam shown in Fig. 3(a) had a nearly circular profile with a diameter of 58 ± 3 μm. The single atom response calculated by the zero-range potential model [24] taking account of the diffraction of the harmonic beam predicts a spot with a diameter of 39 μm, which is smaller than the value experimentally observed. We think that the distortion of the wavefront was caused by both the atomic dipole phases and the ionization of the gas medium for high harmonic generation. Since the atomic dipole phases of high harmonics are proportional to the intensity of the driving laser pulses [25], the wavefront of a generated harmonic has a spatial distribution. The ionized gas also has a refractive index with spatial distribution, which deteriorates the spatial coherence.

When the first grating was set to the 1st-order diffraction, the beam profile of the 17th harmonic became oval-shaped, as shown in Fig. 3(b), because of the diffraction. By directing the second grating at the 1st order, the spectral dispersion of the harmonic was almost compensated for, as shown in Fig. 3(c). The beam diameter at focus was 58 ± 3 μm, which assured the good focusability of the compensator. At the same time, the circular beam profile suggests that the pulse-front tilt was cancelled out by the second grating. This is the first spatial characterization of the pulse-front-tilt compensator.

The numerical ray-trace simulation of the beam profiles shown in Fig. 1(b) demonstrated that the beam area becomes 60 times smaller when the concave mirror is replaced by a toroidal mirror. Therefore, using this light source, we can achieve better spatial resolution.

#121623 - $15.00 USD Received 16 Dec 2009; revised 3 Feb 2010; accepted 4 Mar 2010; published 11 Mar 2010

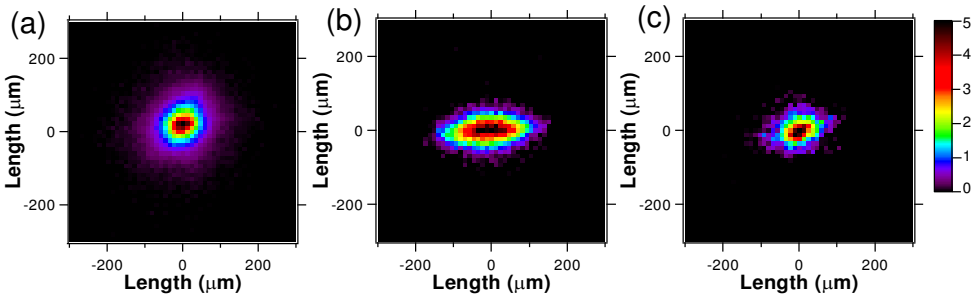

Fig. 3. Beam profiles of the 17th harmonic at the exit of the pulse-front-tilt compensator. (a) A pair of gratings was set to the 0th order. (b) The first grating was set to the 1st order. (c) Both gratings were set to the 1st order.

3.3 Temporal characterization

The diffraction on a grating introduces an optical delay between the adjacent grooves. Thus, the relative optical length depends on the impinging position of the beam, which results in the pulse front tilt inside the beam. In the case of our model, when the grating is irradiated uniformly by a 23rd rectangular pulse, the pulse duration is lengthened to 2 ps. However, in reality, the beam divergence of the high harmonics was smaller than the acceptance angle of the grating, and the spatial distribution was not uniform. Therefore, the cross-correlation measurement of high harmonic pulses with the fundamental laser pulses through the two-photon free-to-free transition shown in Fig. 4(a) gave a pulse duration of the 23rd harmonic pulses of 230 ± 10 fs, when only the first grating was set to the first order.

The compensation produced by the pulse-front tilt was confirmed by setting the second grating to the 1st order. Figure 4(b) shows the cross-correlation and the pulse duration after the compensation was 59 ± 2 fs. Pulse-front-tilt compensation can clearly be observed. We measured the pulse durations of the high harmonic pulses from the 17th to the 23rd harmonics and tabulated them in Table 2. The shortest pulse duration measured in this case was 47 ± 2 fs, when the 21st harmonic was selected. Since the photon number of the 23rd pulses was 3.0 × 10^6 photons/pulse, the peak intensity at focus was 11 MW/cm^2.

To examine the extent of the recompression by the pulse-front-tilt compensator, we measured the original pulse duration of the 23rd harmonic by setting both gratings to the 0th order reflection and then by observing the intensity of the photoelectron peak through the one-photon absorption of the 23rd photons with delay time. Here, we noted not the sideband peaks but the main photoelectron peak by the one-photon transition, because the sideband peak has an indistinguishable contribution from the neighboring peaks (21st or 25th) [21]. The main peak is reduced to produce the sidebands under the simultaneous irradiation by the laser pulses. The cross-correlation trace is shown in Fig. 4(c). The pulse duration was 25 ± 5 fs, which is less than one half of the recompressed pulse. Therefore, the pulse-front tilt still remains after the compensator, as shown in Fig. 4(b).

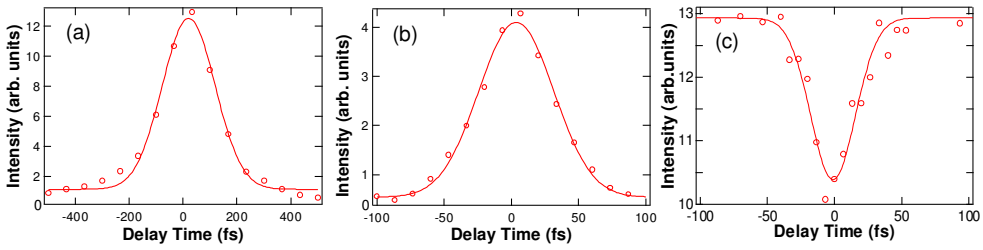

Fig. 4. Temporal cross-correlation functions of the 23rd harmonic pulses with the fundamental laser pulses (a) with only the first grating set to the 1st order, (b) with both gratings set to the 1st order, and (c) with both gratings set to the 0th order. The corresponding pulse durations after the deconvolution are 230 ± 10, 59 ± 2, and 25 ± 5 fs. The solid lines are the fitting results to a Gaussian function.

#121623 - $15.00 USD Received 16 Dec 2009; revised 3 Feb 2010; accepted 4 Mar 2010; published 11 Mar 2010

The pulse broadening from 25 to 59 fs corresponds to a 10-μm difference in the optical path length within the beam. One of the origins of this can be attributed to small displacements of the gratings and the slit from an ideal position, because a 10-μm difference in the optical path is equivalent to the 286-groove change in the irradiation area on the grating. Since the incident angle to the grating is around 71 degrees, only a 170-μm (= 286-grooves) change in the spot size leads to a pulse broadening to 59 fs. This can easily be caused by the misalignment of the incident angle to the gratings or by misalignment of the focal length. In addition, in our experimental setup, the grating mounts wobbled slightly. Thus, we expect that the replacement of the mounts will improve their stability, leading to better compression.

Another origin of the pulse broadening is the imperfect compensation of the angular dispersion by the second grating. In the compensator it is impossible to make each spectral component (wavelength λ) with a diffraction angle β by the first grating impinge on the second grating with the same incident angle β. Therefore, when a harmonic beam incidents on the first grating with an angle α_0, the output angle $\alpha(\lambda)$ from the compensator is no longer constant, α_0, and is approximately expressed as $\alpha(\lambda) = \sin^{-1}(\sin(\alpha_0) + 2(\lambda-\lambda_0)/d)$, where d is the groove pitch and λ_0 is the wavelength of the spectral component with an output angle α_0. Insofar as $\lambda-\lambda_0$ is much smaller than d, $\alpha(\lambda)$ can be assumed to be constant. However, since the lower order harmonics have a more severe angular dispersion, a deviation by $2(\lambda-\lambda_0)/d$ cannot be ignored. In other words, then, the grating with lower dispersion is preferable for pulse-front-tilt compensation. Table 2 shows that the 17th and 19th harmonics have longer pulse durations, which is consistent with the present discussion. This same tendency was also pointed out for the time-compensated monochromator [26].

Table 2. Pulse durations of selected high harmonics

Harmonic order	Photon energy (eV)	Pulse duration (fs)
17	26.5	96 ± 3
19	29.6	80 ± 3
21	32.8	47 ± 2
23	35.9	59 ± 2

Finally, let us briefly mention the pulse duration before the pulse-front-tilt compensator. In Ref. 18, the shortest pulse duration was reported to be 8 fs from 25-fs laser pulses. In addition, our numerical simulations using the zero-range-potential model predicts that the pulse duration of the 21st harmonic can be 15 fs from 30-fs laser pulses, which is shorter than the measured one 25 fs. We think that the longer pulse duration is attributable to relatively higher peak intensity of the laser beam for high harmonic generation. Experimentally, the pulse durations of high harmonic pulses were found to be broader with the peak intensity of the driving laser pulses [27,28]. Temporal and spatial intensity distributions of the laser beam and the ionization of the gas medium during high harmonic generation broaden the pulse durations of the generated high harmonic pulses [27,28]. Since, in the present experimental condition, the peak intensity was set at 5.5×10^{14} W/cm^2 to obtain more high harmonic photons, Ar atoms were ionized significantly. The ionization causes the phase modulation of the laser beam and the diffraction due to the refractive index change, which affect the generation efficiency and the phase-matching condition. Therefore, the measured pulse duration should be longer than expected.

3.4 Comparison among the optical systems

We would like to summarize briefly the specifications of the time-compensated monochromators demonstrated so far in Table 3. The optical system developed in this work has advantage over that of Ref. 17 in focusability. On the other hand, it has lower transmission efficiency 2.6% than that of Ref. 18, 18%. However, the photon numbers on target could be increased to the same order of magnitude just by increasing the driving laser energy to 600 μJ, which can be easily delivered by commercially available laser systems. Therefore, taking

#121623 - $15.00 USD Received 16 Dec 2009; revised 3 Feb 2010; accepted 4 Mar 2010; published 11 Mar 2010

account of the simpler optical configuration, the scheme demonstrated in this work can still be a promising candidate for the pulse-front-tilt compensation.

Table 3. Specifications of the time-compensated monochromators

	Nugent-Grandorf et al.[a]	Poleto et al.[b]	This work
Type of gratings	Spherical and toroidal	Plane	Toroidal
Number of optical components	2	6	2
Maximum throughput (%)	–	18	2.6
Maximum output photon number /pulse	3×10^6	1.3×10^6	4.2×10^6
Pulse energy of a driving laser (mJ)	1.8	0.23	0.60
Shortest pulse duration (fs)	182	8	47

[a] From Ref. 17.

[b] From Refs. 18 and 23.

4. Conclusions

We have developed a pulse-front-tilt compensator, namely time-compensated toroidal grating monochromator, using a pair of toroidal gratings and characterized its focusability and the pulse durations of the output harmonic pulses. 35.9-eV, 3.0×10^6 harmonics photons with a pulse duration of 59 ± 2 fs could be focused into an area with a diameter of 58 ± 3 μm. The peak intensity reached 11 MW/cm^2. In spectroscopy, this light source offers advantages over the combination of multilayer mirrors and thin metal foils that has often been implemented, in that: 1) The purity of the wavelength is better, because other harmonics are completely eliminated by a slit; 2) Pump or probe photon energies are tunable, although the wavelength is fixed in multilayer mirrors; and 3) Thin metal foils are not needed to stop the fundamental laser pulse, which improves the throughput of the system. For these reasons, the pulse-front-tilt compensator will become a versatile tool for XUV time-resolved spectroscopy and nonlinear optics.

Acknowledgments

TS is supported by a Grant-in-Aid for Scientific Research (A) from the Japan Society for the Promotion of Science, Murata Science Foundation, and the MATSUO FOUNDATION.

#121623 - $15.00 USD Received 16 Dec 2009; revised 3 Feb 2010; accepted 4 Mar 2010; published 11 Mar 2010